

NIST Special Publication 260-165

**Certification of Standard Reference
Material[®] 5000
Calibrated Overlay Wafer Standard**

Michael T. Stocker
Richard M. Silver
Ravikiran Attota
Jay S. Jun

This publication is available free of charge from:
<https://doi.org/10.6028/NIST.SP.260-165>

NIST
**National Institute of
Standards and Technology**
U.S. Department of Commerce

NIST Special Publication 260-165

**Certification of Standard Reference
Material[®] 5000
Calibrated Overlay Wafer Standard**

Michael T. Stocker
Richard M. Silver
Ravikiran Attota
Physical Measurement Laboratory

Jay S. Jun
Manufacturing Engineering Laboratory

This publication is available free of charge from:
<https://doi.org/10.6028/NIST.SP.260-165>

January 2007



U.S. Department of Commerce
Carlos Gutierrez, Secretary

National Institute of Standards and Technology
William A. Jeffrey, NIST Director

Certain commercial entities, equipment, or materials may be identified in this document in order to describe an experimental procedure or concept adequately. Such identification is not intended to imply recommendation or endorsement by the National Institute of Standards and Technology, nor is it intended to imply that the entities, materials, or equipment are necessarily the best available for the purpose.

National Institute of Standards and Technology Special Publication 260-165
Natl. Inst. Stand. Technol. Spec. Publ. 260-165, 18 pages (January 2007)
CODEN: NSPUE2

This publication is available free of charge from:
<https://doi.org/10.6028/NIST.SP.260-165>

NIST SP 260

SRM 5000 Calibrated Overlay Wafer Standard

M.T. Stocker, R.M. Silver, J. Jun, R. Attota

Introduction: Semiconductor devices are created by exposing successive patterns onto a photosensitive resist spun onto a wafer. The proper functioning of the device depends on, among many things, how well each successive layer is aligned to the previous layers. The measure of how well one exposure pattern aligns with the next is termed “overlay” (OL). Optical OL measurements are very complex and involve looking through multiple layers of a process stack. Many factors contribute to the final accuracy of an overlay measurement, including wafer and tool related errors.

In a collaborative effort with International Sematech (ISMT) and the Overlay Metrology Advisory Group (OMAG), the National Institute of Standards and Technology (NIST) has designed and is introducing an industry relevant overlay wafer calibration standard, SRM 5000. Its intended use is to establish accuracy and traceability on various optical overlay metrology tools. It can be used on any type of overlay metrology tool (Scanning Electron Microscope (SEM), Atomic Force Microscope (AFM), Optical Microscope, etc.) with the appropriate sample holding capabilities and proper magnification to see and measure the calibrated targets.

Physical Description: SRM 5000 is a 200 mm double-etched silicon wafer containing various research and calibration targets. The wafer contains 93 dies, each die measuring 17.6 mm in X by 16.0 mm in Y, with a 17.6 mm pitch in the X-direction and a 16.0 mm pitch in the Y-direction. A single die is broken into 4 quadrants: QI, QII, QIII and QIV. QIII is further divided into four subquadrants: SQ1, SQ2, SQ3 and SQ4.

Figure 1 shows a progressively exploded view of the SRM 5000. QIII contains the relevant overlay calibration targets. The “5 to -5” labeling on the left and bottom of the wafer denote Die position. A limited number of Frame-in-Frame (FF) and Bar-in-Bar (RR) targets within QIII of the center die (Die 00-00) are calibrated. Ten total OL targets were selected to calibrate; five FF targets from cell #8 and five RR targets from cell #9. The FF targets are located in SQ3 and the RR targets are located in SQ4. Both SQ3 and SQ4 contain 10 cells. Each cell consists of two rows of targets; one row with the x-offset and the other with the y-offset. There are a total of 27 OL offsets in each row of targets, ranging from $-0.175\ \mu\text{m}$ to $+0.175\ \mu\text{m}$. Figure 2 shows a further exploded view of SQ3, illustrating the relevant labeling on the wafer.

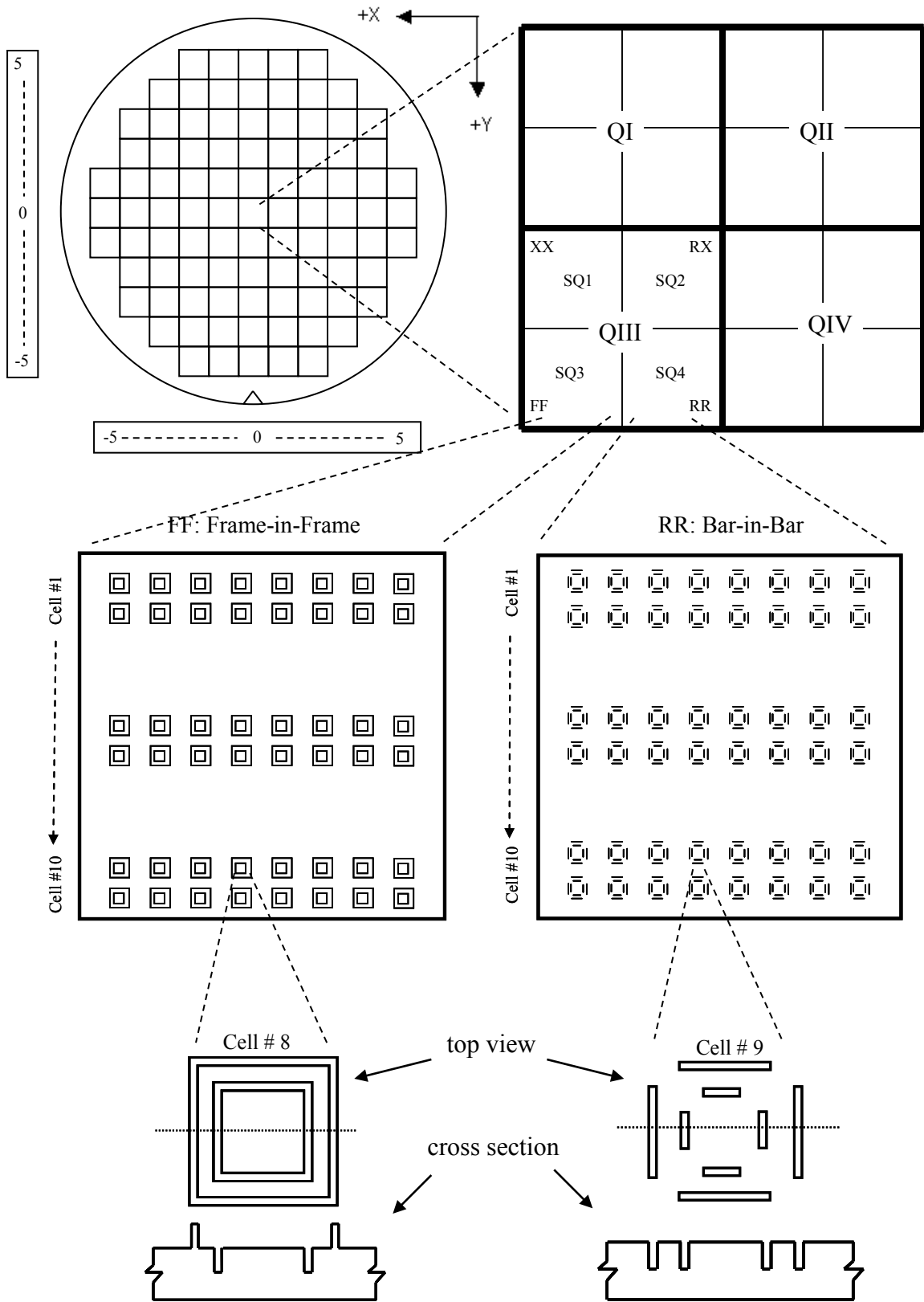


Figure 1 - Exploded view of the center die of the SRM 5000

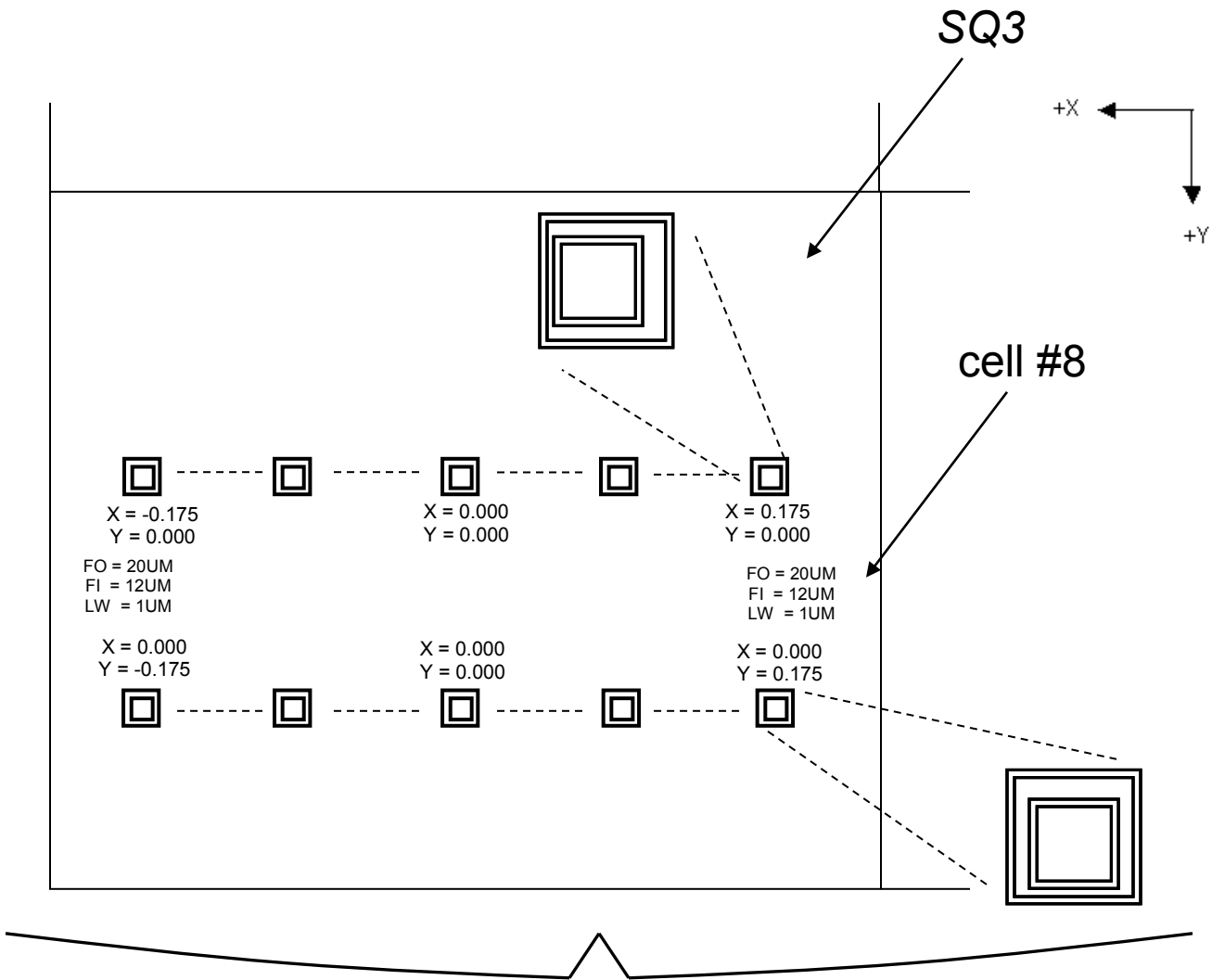


Figure 2 – Illustration of relevant labeling in Sub-quadrant 3

Type	Die	Quadrant	Sub-quadrant	Cell	Offset
FF	00-00	III	3	8	X=+0.100 μ m
FF	00-00	III	3	8	X=+0.030 μ m
FF	00-00	III	3	8	X=+0.000 μ m
FF	00-00	III	3	8	X=-0.030 μ m
FF	00-00	III	3	8	X=-0.100 μ m
RR	00-00	III	4	9	Y=-0.050 μ m
RR	00-00	III	4	9	Y=-0.010 μ m
RR	00-00	III	4	9	Y=+0.000 μ m
RR	00-00	III	4	9	Y=+0.010 μ m
RR	00-00	III	4	9	Y=+0.050 μ m

Table 1 – FF and RR offsets that are calibrated

Table 1 lists the offsets calibrated in the FF and RR target sets. The FF targets are two-level structures and the RR targets are single-level structures as seen in the cross section at the bottom of Figure 1. The outer frame of the FF targets has a positive polarity (protruding upward from the substrate) and the inner frame of the FF targets has a negative polarity (etched into the substrate). Both the inner and outer frames of the RR targets have a negative polarity. The heights and depths, relative to the substrate, of the structures making up each OL target are on the order of 500 nm. The selected FF targets have an outer frame dimension of 20 μm , an inner frame dimension of 12 μm , and a critical dimension (CD) of 1.0 μm . The selected RR targets have an outer frame size of 20 μm , an inner frame size of 8 μm , and a CD of 0.5 μm . The dimensions of the inner and outer frames of the FF and RR targets are measured from outer-edge to outer-edge. As seen in Figure 2, the target labeling is readable left-to-right when the wafer notch is facing the user. In this reference frame, the x-axis is parallel to the labeling and the y-axis is perpendicular to labeling. A positive x-offset for the FF targets corresponds to a left shift of the inner frame relative to the outer frame. For the RR targets, a positive y-offset corresponds to a downward shift of the inner frame relative to the outer frame. A xy coordinate marker in figures 1 and 2 elucidates the direction of the shift of the inner frame relative to the outer frame for a positive offset target with respect to the overall wafer layout.

Calibration Strategies: There are different strategies one can implement in using an artifact to calibrate a tool or a tool set [1]. It can be used as 1) a calibration artifact or 2) a verification artifact. The choice between strategies can have a measurable effect on the final measurement uncertainty of the metrology tool(s) being calibrated. In the first approach, using the NIST SRM 5000 as a calibration artifact, the mean of multiple measurements is used to calibrate the metrology tool outputs. Depending on the nature of the errors present in the user's measurement system, this can mean a simple linear scale adjustment or a more complex, possibly non-linear correction. In the end, with this method, the user's uncertainty budget would include at least the entire NIST uncertainty, the end-user's repeatabilities, and the uncertainty of any corrections applied to their metrology tool. To arrive at a Combined Uncertainty (CU) for this approach, the NIST 1 σ uncertainty value would be combined in Root Sum Square (RSS) with all of the end-user's sources of uncertainty.

Alternatively, in the second approach, an independent and comprehensive calibration can be performed and the NIST SRM 5000 serves as a verification artifact. Here, the tool is completely evaluated by measuring and/or scientifically estimating each relevant component of uncertainty and applying either a Type A or Type B treatment to each. Type A uncertainty components are those that can be evaluated by statistical means, resulting in a mean and variance. Type B components are those whose variances are estimated based on sound scientific judgement. The general approach to determine and express measurement uncertainty is spelled out in the U.S. Guide to the Expression of Uncertainty in Measurement (GUM). We refer the reader to the GUM for a more comprehensive discussion on the evaluation and expression of measurement uncertainty [2]. This comprehensive calibration approach has the advantage of avoiding certain components of the NIST uncertainty budget, such as our components due to repeatability

and scale. After a tool has been calibrated, the SRM 5000 is then used to verify the effectiveness of the calibration. The CU for this method will include the uncertainty in establishing traceability, repeatabilities, all of the other components specific to the user's system, and finally a term to account for the difference between the NIST calibrated values of the SRM 5000 and the final measurements from the user's Overlay Metrology Tool (OMT). Again, all of these components are combined in RSS to arrive at a CU.

To evaluate a tool set, each tool would be calibrated independently of the others, applying either one of the strategies discussed above. The SRM 5000 is then measured on each of the tools to determine a tool set mean and variance. This allows for an unknown wafer to be measured without regard to knowing the specific tool. The formulas to combine the individual measurements into a tool set calibration are available in Reference [1]. To determine the CU for the tool set, the tool set variance is combined in RSS with the rest of the relevant uncertainty components.

Certification Technique: The NIST OMT was the sole instrument used in calibrating the SRM 5000's. The OMT, specifically designed to do high-accuracy overlay measurements, is a full-field CCD based 2-d overlay metrology optical microscope. For these measurements, it was operated in a bright field reflection mode using green light ($\lambda = 546 \text{ nm}$) at a 50X magnification, corresponding to a $43.0 \mu\text{m}$ field of view (FOV). In our overlay algorithms we use the following window dimensions: FF – $4.1 \mu\text{m} \times 2.1 \mu\text{m}$ and RR – $6.2 \mu\text{m} \times 2.1 \mu\text{m}$. See Figure 3 for a schematic of the dimensions of one of the four identical windows needed to do an overlay calculation.

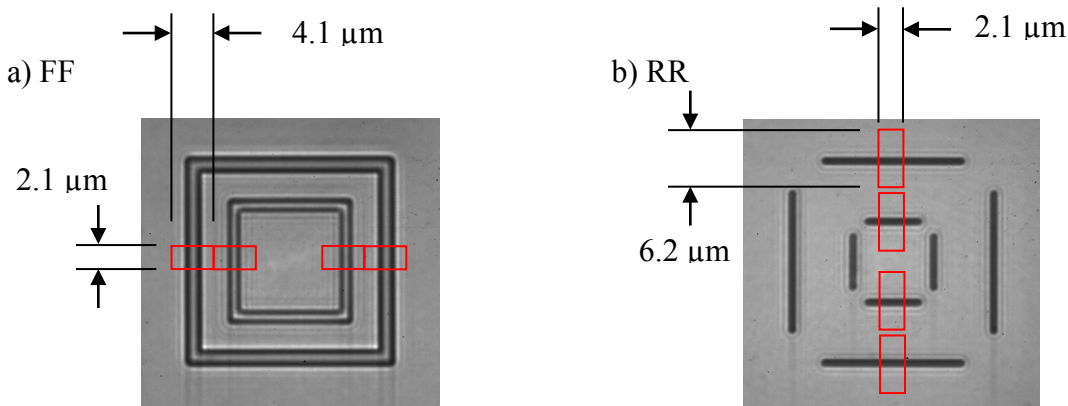


Figure 3 – Window dimensions for FF and RR targets

Each wafer was measured at least 5 times on several days to adequately sample the reproducibility of the measurement system. A measurement of a given target within the total measurement sequence of a wafer consisted of individual auto-center and auto-focus operations, repeated three times at 0° and three times at 180° , for a total of six independent dynamic measurements of a target on any given day and a complete measurement total of at least thirty measurements on that target. The difference between the 0° and 180° measurements gives us the Tool Induced Shift (TIS), which we monitor as an indication of a properly aligned tool. TIS is operationally defined as

$$TIS = (OL_0 - OL_{180})/2$$

The average of the 0° and 180° measurements gives us the TIS Corrected Mean (TCM). The average TCM is the calibrated value that is reported.

E. Kornegay, formerly of the Manufacturing Engineering Laboratory (MEL), and R. Attota, an independent consultant to the MEL, were responsible for development of the OMT. Algorithms for determining and reporting the overlay registration values [3] were programmed by J. Jun of the MEL and an independent set of OL algorithms were developed by R. Attota to confirm various aspects of our uncertainty budget. Measurements and statistical analysis were performed by M. Stocker of the MEL. Statistical support was provided N. F. Zhang of the Information Technology Laboratory. This work was performed under the technical supervision of R. Silver of the MEL.

Control Chart: Statistical control of the measurement process was maintained throughout the SRM calibrations by measuring a control sample on regular intervals. The control sample is a wafer from the same wafer boat, assumed to have the same physical and optical material properties as the wafers being calibrated. This is important in that a control sample should be as equally sensitive to process shifts as the samples being calibrated. The same features that were calibrated on the SRM wafers were measured on the control wafer throughout the entire calibration process. The FF target control chart is shown in Figure 4 and the RR target control chart is shown in Figure 5.

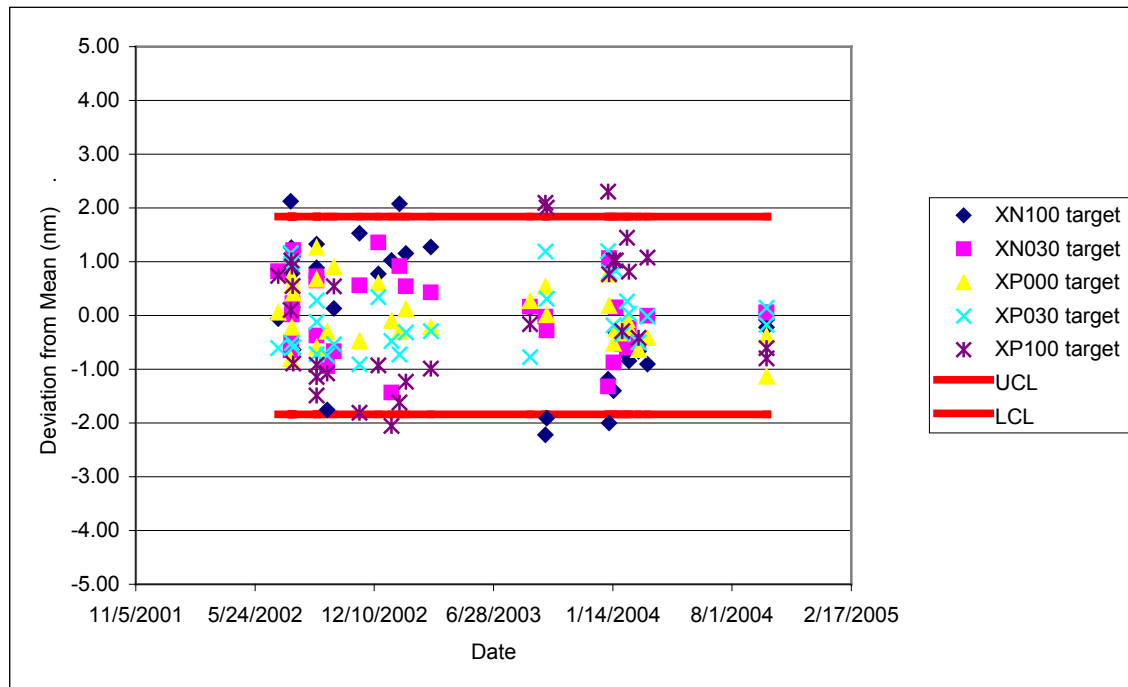


Figure 4 – FF control chart (UCL – Upper Control Limit, LCL – Lower Control Limit)

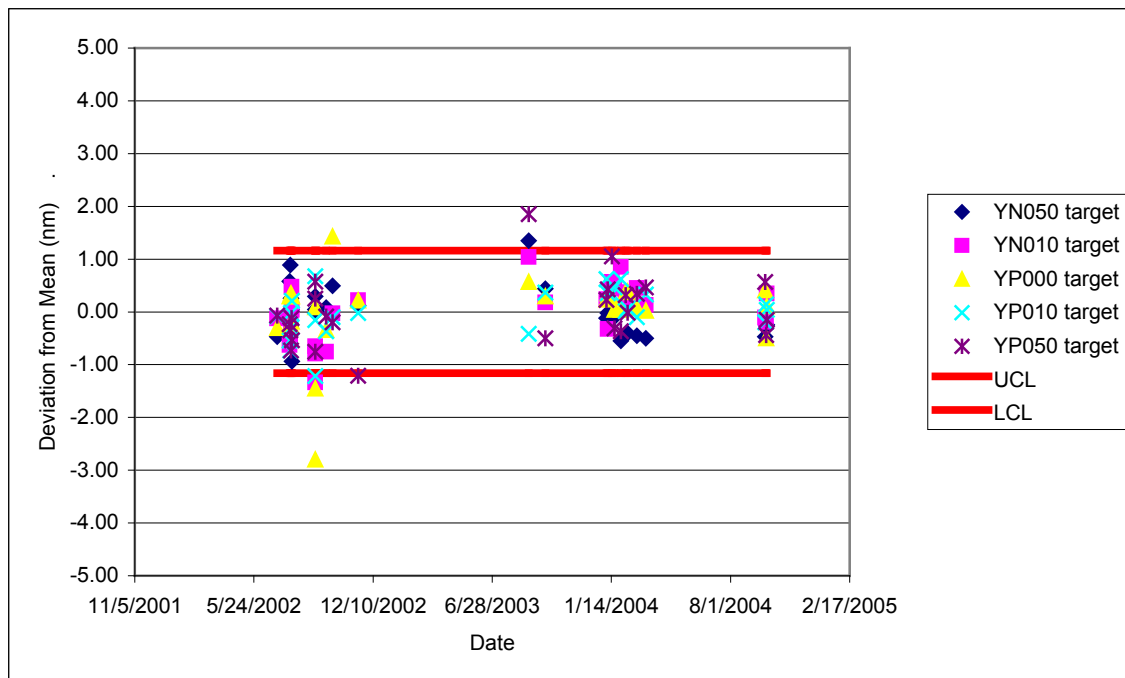


Figure 5 – RR control chart (UCL – Upper Control Limit, LCL – Lower Control Limit)

Expiration of Certification: The certification of the SRM 5000 is valid indefinitely, within the measurement uncertainty specified, provided the SRM is handled and stored in accordance with the instructions given in this certificate (see Instructions for care and cleaning). Periodic recertification is not required; however, this certification will be nullified if the SRM is damaged, contaminated, or modified.

The support aspects involved in the preparation, certification, and issuance of this SRM were coordinated through the NIST Standard Reference Materials Group by M. Cronise.

Instructions for Care and Cleaning: Care must be exercised when handling and storing the SRM 5000. The process stack for this SRM wafer is double-etched silicon. Nothing must come in contact with the surface of the wafer. The wafer must be stored in a clean stable environment, preferably inside a wafer shell in a Class 100 or better cleanroom. Any contamination on the wafer within the optical proximity of the calibrated targets, typically on the order of 5 μm for these targets, will render the calibration void. This wafer is not intended to be separated into individual dies, doing such will void the calibration.

Calibration Uncertainty: The guidelines and recommendations set forth in the US Guide to the Expression of Uncertainty in Measurement (GUM) were used to derive the following SRM 5000 uncertainty budget. The GUM is widely followed and recognized by the international measurement and metrology institutions abroad. The SRM 5000 measurement uncertainty components and their values are listed in Table 2 and then further discussed below. Again, Type A uncertainty components are those that can be

evaluated by statistical means and Type B components are estimated based on sound scientific judgement. For a more thorough discussion on measurement uncertainty, we refer the reader to the GUM [2].

Number	Uncertainty Component Description	Type	Standard Uncertainty, u_c , (nm)			
			$ \text{OL} \leq 63 \text{ nm}$		$63 \text{ nm} < \text{OL} \leq 125 \text{ nm}$	
			FF	RR	FF	RR
1	Measurement Repeatability	A	actual	actual	actual	actual
2	Control Sample	B	0.30	0.25	0.60	0.50
3	Metrology Shift Correction	B	actual	n/a	actual	n/a
4	Scale	B	0.20	0.20	0.40	0.40
5	Pixel Placement / Response	B	1.10	1.10	1.10	1.10
6	TIS Correction	B	0.50	0.50	0.50	0.50
7	Computational (algorithm)	A	0.10	0.10	0.20	0.20
8	Computational (profile)	B	0.15	0.15	0.30	0.30
9	Computational (implementation)	B	0.10	0.10	0.20	0.20
10	Wafer-induced Shift	B	0.00	0.00	0.00	0.00

Table 2 – Summary of relevant uncertainty components. All values are in nm.

The SRM 5000 uncertainty budget includes the components listed in the table above. The uncertainty budget was divided into four groups, based on 1) the magnitude of the measured overlay and 2) the type of OL target. This approach was used to minimize the effects of certain errors on smaller overlay values ($\text{OL} \leq 63 \text{ nm}$) as well as to minimize the effects of certain errors on RR targets versus FF targets. In general, the single level RR targets were less susceptible to many of the errors encountered in the calibration process. Each of the individual uncertainty components is discussed in greater detail below.

- 1) *Measurement Repeatability* – The uncertainty due to the repeatability of the overlay system was evaluated by using the actual standard deviation values of the repeated measurements of each individual target. The 1σ repeatability was typically better than 1 nm. This approach was used, instead of assigning a worst-case uncertainty, to keep from unnecessarily inflating the uncertainty of targets with smaller repeatabilities.

$$u(\text{repeatability}) = \text{actual calculated value for each target is used}$$

- 2) *Control Sample* – A control wafer was measured to monitor the integrity of the measurement system throughout the entire calibration process. This is, in fact, a measurement of the longer-term reproducibility of the system. In the middle of the measurements for this set of SRM calibrations, a small metrology shift was identified which needed to be accounted for in the uncertainty budget.

For FF targets:

$$u(\text{control}) = \begin{cases} 0.30 \text{ nm, if } OL \leq 63 \text{ nm} \\ 0.60 \text{ nm, if } 63 \text{ nm} < OL \leq 125 \text{ nm} \end{cases}$$

For RR targets:

$$u(\text{control}) = \begin{cases} 0.25 \text{ nm, if } OL \leq 63 \text{ nm} \\ 0.50 \text{ nm, if } 63 \text{ nm} < OL \leq 125 \text{ nm} \end{cases}$$

- 3) *Metrology Shift Correction* – This uncertainty component arises from mathematically adjusting the FF data to center the OL result between the two different tool modes that we sampled in the observed Metrology Shift described above. The 1σ value for this uncertainty component is typically on the order of 0.3 nm or less. There was no measurable effect from the shift on the RR data.

$u(\text{msc})$ = actual calculated value for each target is used

- 4) *Scale Calibration* – To establish traceability, a known artifact was measured on the Overlay system to calibrate the optics/camera combination. The traceable artifact was a NIST SRM 2800 Microscope Magnification Standard [4]. The uncertainty propagated through to our overlay measurements as a result of the uncertainty in the traceable artifact is negligible. However, in repeating the measurement of this artifact on the overlay system, a distribution of calibration factors was created, from which a measurable component of uncertainty was determined. Our effective scale factor is on the order of 41.15 ± 0.20 nm/pixel.

At first glance, the magnitude of this component may appear a little small. Considering the 0.2 nm/pixel variation in conjunction with the size of our OL offset in pixels, we arrive at the uncertainty values listed below. In the end, the scale only contributes uncertainty over the differential distance between the calculated centerlines. The justification behind the treatment of the scale error in this way lies in the fact that the overlay target centerline calculations are correlated (they are performed on the exact same pixel reference frame).

$$u(\text{scale}) = \begin{cases} 0.20 \text{ nm, if } OL \leq 63 \text{ nm} \\ 0.40 \text{ nm, if } 63 \text{ nm} < OL \leq 125 \text{ nm} \end{cases}$$

- 5) *Pixel Placement and Response (ppr)* – The pixel pitch of a CCD array is never perfect. This component accounts for the non-uniform pixel spacing and response of the CCD on the overlay measurement system. It was evaluated by stepping an appropriate pitch pattern through the FOV and applying a 1-D self-calibration algorithm [5].

This algorithm is shown schematically in Figure 6. P_n represents the pitch of the pitch pattern. X_n is the location in the FOV of our microscope. At time $t=0$, every pitch P_0 to P_{n-1} is measured in the FOV in their respective locations, X_0 to X_{n-1} . At time $t=1$, the pitch pattern is shifted to the right and measured again. Now, P_0 has been measured in locations X_0 and X_1 . A calibration factor γ_1 can be calculated by taking the ratio of the pitch P_0 measured at location X_1 divided by the pitch P_0 measured at location X_0 . For any given location X_n , the calibration factor can be written as $\gamma_n = P_{n-1}(X_n)/P_{n-1}(X_{n-1})$.

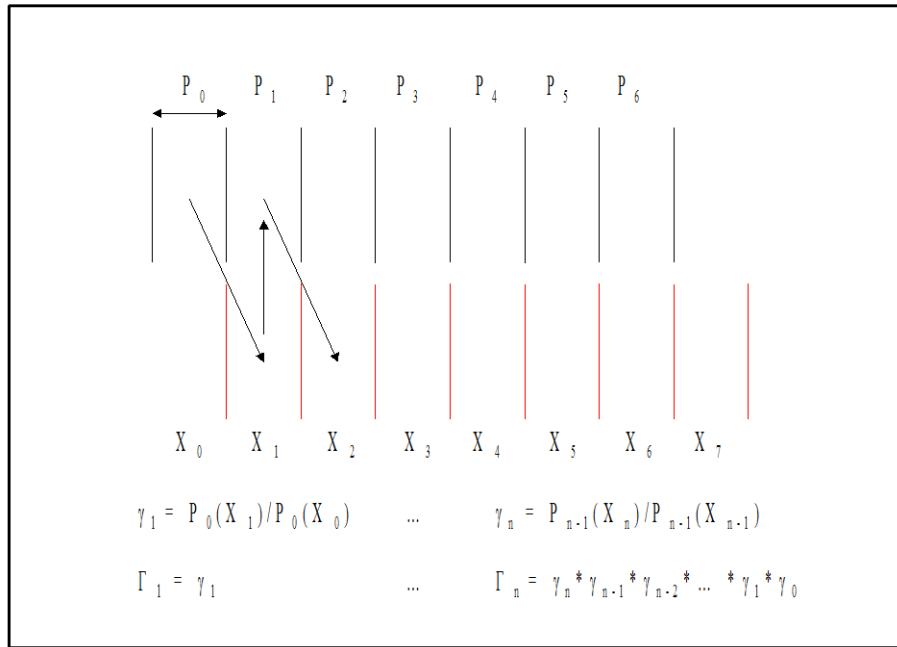


Figure 6 – Diagram of 1-d self-calibration algorithm

The intent of this algorithm is to relate any location X_n to the original location X_0 . To achieve this, another factor, Γ_n , is introduced. To relate location X_1 to location X_0 , $\Gamma_1 = \gamma_1$. To relate any given location X_n to the original location X_0 , $\Gamma_n = \gamma_n * \gamma_{n-1} * \gamma_{n-2} * \dots * \gamma_1 * \gamma_0$. In practice, to evaluate higher frequency pixel pitch and pixel response distortions, the pitch pattern is stepped in fractions of the integer pitch. It is important to note that, having done this, not all of the data relates back to the original position in the FOV. Now, data acquired in each of the inter-pitch positions is related back to the closest previous integer position of the pitch pattern. From this procedure, a distribution of correction values versus

position in the FOV is built up, as seen in Figure 7. It is from the variance in these corrections that we estimate our standard uncertainty for this effect.

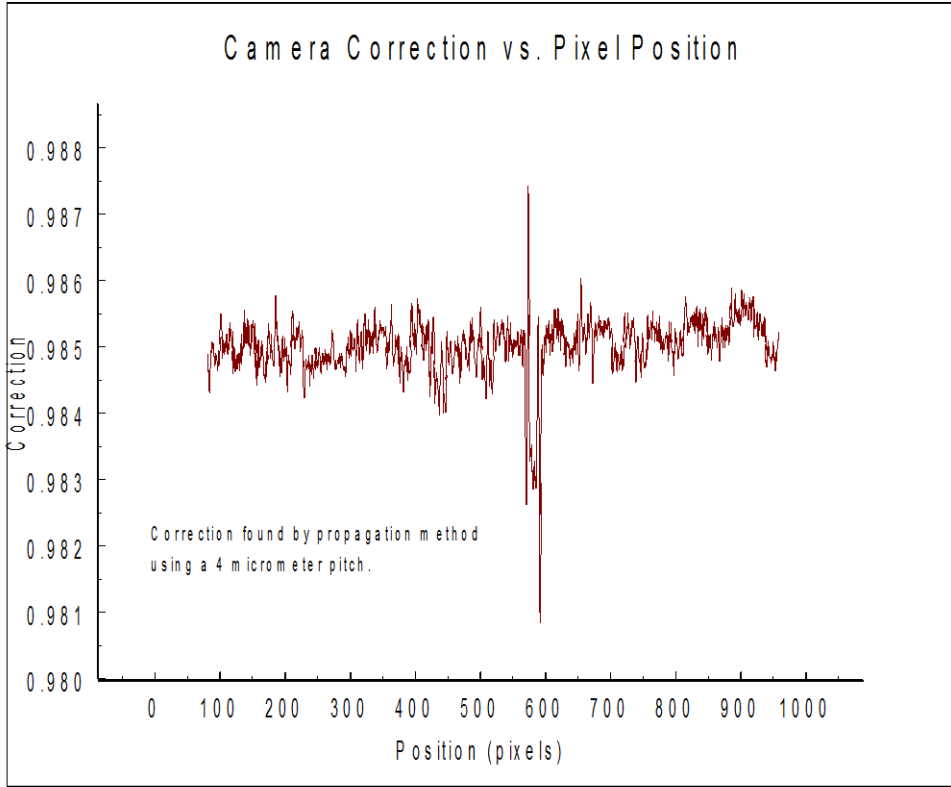


Figure 7 – Plot of CCD pixel pitch calibration factors versus position

$$u(ppr) = \begin{cases} 1.10 \text{ nm, if } OL \leq 63 \text{ nm} \\ 1.10 \text{ nm, if } 63 \text{ nm} < OL \leq 125 \text{ nm} \end{cases}$$

- 6) *TIS Correction* – The effectiveness of the TIS correction which we apply to our OL measurements is taken into consideration in this uncertainty component. In this case, we chose to implement a worst-case value to cover the entire spectrum of overlay values. Our estimates were made large enough to include any TSI (Tool Sample Interaction) that may have been present in our measurements.

$$u(TIS) = \begin{cases} 0.50 \text{ nm, if } OL \leq 63 \text{ nm} \\ 0.50 \text{ nm, if } 63 \text{ nm} < OL \leq 125 \text{ nm} \end{cases}$$

- 7) *Computational (algorithm)* – Determining the OL value involves using complicated image processing and edge detection algorithms. The algorithms are typically developed for best repeatability and robustness. Interpolation, filtering,

and window size are just a few of the algorithm inputs. Once a repeatable and robust algorithm is achieved, then the effects of the different input parameters on the accuracy of the result must be accounted for. A parametric study was performed around the standard inputs to our OL algorithm and the spread of these results were used in estimating this source of uncertainty.

$$u(\text{algorithm}) = \begin{cases} 0.10 \text{ nm, if } OL \leq 63 \text{ nm} \\ 0.20 \text{ nm, if } 63 \text{ nm} < OL \leq 125 \text{ nm} \end{cases}$$

- 8) *Computational (profile)* – Separate from the different parameters that are involved in the OL calculation is a choice regarding what portion of the profile to perform the OL calculation on. One can, in principal, use any portion of the profile, from the entire profile to a very small slice, to do the OL calculation. When the entire profile is used it is referred to as a complete profile. When any amount less than the entire profile is used, it is referred to as a truncated profile.

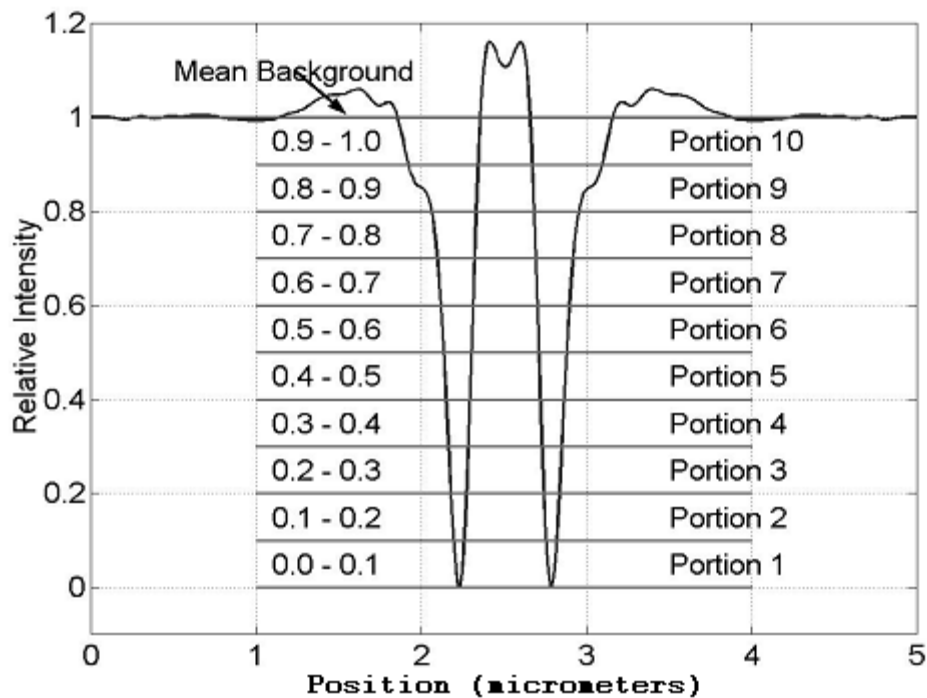


Figure 8 – Levels of Truncation on one leg of an OL target.

We have studied the effects of profile truncation on the calculated OL. It was concluded that some regions of the profile are less sensitive to proximity and optical system errors. This uncertainty component is intended to account for differences observed in the OL calculations as a function of truncation. Figure 8 illustrates what

is meant by profile truncation. We refer the reader to Reference [6] for a more in depth discussion on the effects of profile truncation on OL calculations.

$$u(\text{profile}) = \begin{cases} 0.15 \text{ nm, if } OL \leq 63 \text{ nm} \\ 0.30 \text{ nm, if } 63 \text{ nm} < OL \leq 125 \text{ nm} \end{cases}$$

- 9) *Computational (implementation)* – Two separate and independent OL software codes were developed at NIST. The older more fully qualified OL code was used in the formal calculation and reporting of the OL registration values in the SRM 5000 calibrations. The second independently developed code was used to assist in evaluating different aspects of the OL uncertainty budget. Effort was invested to ensure agreement between the two OL codes. Any remaining disagreement between the two OL codes is reflected here.

$$u(\text{implementation}) = \begin{cases} 0.10 \text{ nm, if } OL \leq 63 \text{ nm} \\ 0.20 \text{ nm, if } 63 \text{ nm} < OL \leq 125 \text{ nm} \end{cases}$$

- 10) *Wafer-induced Shift* – Wafer-induced shift, or WIS, is a measure of the sample asymmetry. This relates to any errors introduced as a result of an imperfect sample, which could be attributed to physical geometry or material properties. For example, Figure 9 shows a cross-section of a FF target where the sidewall angle on the inside of the left outer feature is not vertical. This type of non-perfect geometry will introduce a WIS. To assess this aspect of our uncertainty, we have gone through the process of developing a “feature” reversal technique specifically intended to evaluate sample asymmetry. In Reference [7], we describe this mapping methodology, which enables us to separate the effects of TIS and WIS on an OL registration measurement. This mapping process involves performing “feature” reversals of one leg of an overlay target throughout the FOV. Residual plots are created by subtracting the 0° profile from the 180° profile at every place in the FOV that was sampled as part of the optical map. To this point, no definitive uncertainty contribution to the OL offset has been attributed to sample asymmetry. Subsequent analysis using a SEM and an AFM has not identified a measurable sample asymmetry, which would contribute an error in an OL measurement.

$$u(\text{WIS}) = 0 \text{ nm}$$

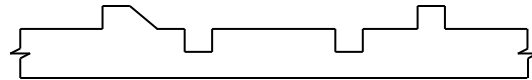


Figure 9 – FF target cross-section with WIS

Calibration Traceability: Traceability to the meter was established through repeated measurements of a NIST SRM 2800 Microscope Magnification Standard [4] on the OMT. This SRM 2800 was previously measured on the Precision Engineering Division Linescale Interferometer, which is our practical realization of the meter. These measurements were the basis for determining the scale factor of the microscope, which includes the optics and the CCD. Figure 10 is a picture of the SRM 2800 as viewed in our FOV. It was stepped through the FOV in 4 different angular orientations, allowing us to calculate a stable average calibration factor for our microscope system.

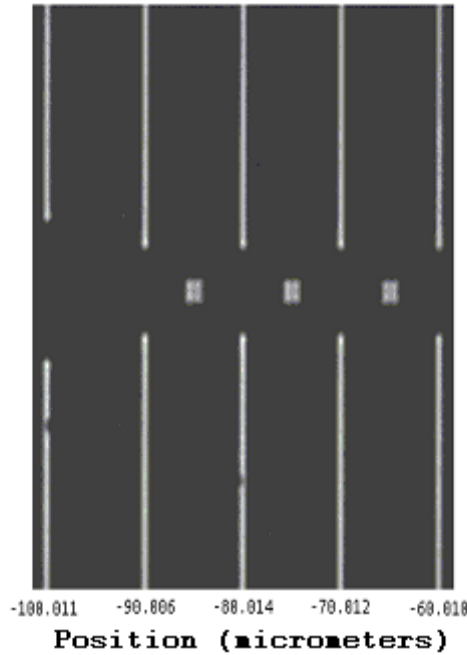


Figure 10 – Image at 100X of the SRM 2800 used to calibrate the camera/microscope scale.

Combined Uncertainty: All of the 1σ uncertainty components described above are added in quadrature to arrive at a CU for each of the 10 calibrated targets on the wafer. Additionally, a coverage factor (k) of two is applied to each of the calculated combined uncertainties. This result, the Expanded Uncertainty ($k=2$), is the uncertainty reported with each of the calibrated values.

References:

- [1] Richard M. Silver, Michael T. Stocker, Ravikiran Attota, Michael Bishop, Jau-Shi J. Jun, Egon Marx, Mark P. Davidson, and Robert D. Larrabee, "Calibration strategies for overlay and registration metrology", Proc. SPIE Vol. 5038, p. 103-120, Metrology, Inspection, and Process Control for Microlithography XVII, 2003
- [2] "American Nat'l Stand. for Calibration – U.S. Guide to the Expression of Uncertainty in Measurement", ANSI/NCSL Z540-2-1997, published by NCSL International, ISBN 1-58464-005-7
- [3] Richard M. Silver, Jau-Shi J. Jun, Edward Kornegay, and Robert D. Morton, "Comparison of edge detection methods using a prototype overlay calibration artifact", Proc. SPIE Vol. 4344, p. 515-529, Metrology, Inspection, and Process Control for Microlithography XV, 2001
- [4] J. Potzick, "New NIST-Certified Small Pitch Standard," 1997 Measurement Science Conference, Pasadena, Calif. (1997)
- [5] S. Fox, E. Kornegay, and R. Silver, "Characterization of Imaging Optics and CCD Cameras for Metrology Applications", ULSI Conf. Proc., NIST 2000
- [6] R. Attota, R. Silver, M. Stocker, E. Marx, Jau-Shi J. Jun, M. Davidson, R. Larrabee, "A new Method to Enhance Overlay Tool Performance", Proc. SPIE Vol. 5038, p.428-436, Metrology, Inspection, and Process Control for Microlithography XVII, 2003
- [7] R. Silver, R. Attota, M. Stocker, Jau-Shi J. Jun, E. Marx, R. Larrabee, B. Russo, and M. Davidson, "Comparison of Measured Optical Image Profiles of Silicon Lines with Two Different Theoretical Models", Proc. SPIE Vol. 4689, p. 409-429, Metrology, Inspection, and Process Control for Microlithography XVI, 2002